Interferometric SAR and laser scan data integration

D. Colombo[1], F. Coren[2] and P. Sterzai[2]

[1] *Tele-Rilevamento Europa - T.R.E. s.r.l., c/o Dip. Elett. Inform. Politecnico, Milan, Italy*
[2] *Istituto Nazionale di Oceanografia e di Geofisica Sperimentale - OGS, Trieste, Italy*

(Received May 17, 2004; accepted September 9, 2004)

ABSTRACT This paper describes the potential of a synergistic use of three remote sensing technologies: an airborne laser scanner, high-resolution optical data and satellite radar acquisitions. This methodology allows one to describe the terrain surface in extreme spatial detail and to extract information about possible surface deformation phenomena. More precisely, we generate geocoded products derived from the integration of airborne laser scan data, ortho-images and satellite interferometric data. This synergistic framework allows one to describe the territory in a multidimensional way. The spatial component is given by a high-accuracy digital elevation model from the laser scan acquisition; radiometric attributes are described by the high-resolution digital ortho-images, while the characterization of local dynamics is provided by the application of the so-called Permanent Scatterers technique, a new technique recently developed by the Politecnico of Milan, capable of detecting and monitoring possible range variations of a sub-set of privileged radar targets, on ground. A specific study area to build up a case history has been identified. The test-site is the historic town of Palmanova in Italy.

1. Introduction

In the last decade, a number of leading-edge remote sensing technologies has matured from the research stage to applications. Two are creating a major impact on the community of final-users, namely: the airborne laser scan and synthetic aperture radar interferometry (InSAR), in particular the Permanent Scatterers (PSs) technique. Laser scan is an innovative technique addressed to topographic data collection. This method is challenging the common aerial photogrammetry or the more recent satellite stereogrammetry for land surveying. Indeed, Laser Detection and Ranging (LIDAR) has gained considerable acceptance in both the scientific and commercial communities as a tool for topographic measurement and, despite its recent emergence, has already become an standard-industrial-tool for collecting high-resolution topographic data.

The National Institute of Oceanography and Applied Geophysics (OGS) and Helica Laser Terrain Mapping have undertaken an extensive use of this methodology operating an Optech 3033 laser scan. The system used is an ALTM 3033 laser mapping designed to generate topographic maps. In this paper, the principles and technical issues related to this technology, as well as its precision, are presented.

The PS technique can be considered the evolution of conventional InSAR analyses. The method has already gained considerable attention in land-monitoring applications and it is

becoming the standard *de facto* for the to recovery of high-quality measurements of ground and building deformation over large areas.

By integrating LIDAR digital elevation model (DEM) and PS maps, as well as optical ortho-images, a multidimensional picture of the area of interest can be obtained. Spatial properties (from LIDAR DEM), radiometric attributes (from ortho-images) and motion components (from PS data) can be then imported into a GIS framework. This paper describes a case history of such a fusion.

2. The laser scan system

The airborne laser scan (ALS) terrain mapping is a method that allows one to reconstruct, with high accuracy and high resolution, the local topography of an area of interest (Ackermann, 1999; Hill *et al.*, 2000). The system is based on an instrument transmitting laser pulses while scanning a swath of terrain, usually centred on, and co-linear with, the flight path of an aircraft or a helicopter in which the instrument is mounted. More precisely, the system consists of an infrared laser, an inertial navigation system (INS), receiver optics and electronics, and a control rack.

The infrared laser emits narrow optical pulses which a scanning mirror directs perpendicularly to the flight path providing coverage to either side of the flight direction; the forward motion of the aircraft provides coverage in the direction of flight. The system measures round-trip travel times of the laser pulses from the aircraft to the ground. The time intervals are converted into range measurements, and the position of the aircraft at the instance of firing the pulse is determined (Baltsavias, 1999) by differential Global Positioning System (GPS). The roll, pitch and yaw (attitude) of the aircraft are measured by the inertial navigation system unit at a frequency of 200 Hz. The ALTM 3033 laser we operate can measure up to 33000 laser pulses per second at a mirror scan angle of up to 20 degrees either side of the vertical. Angular positions of the laser beam are combined with aircraft attitude values determined by the INS based on three laser ring gyroscopes to achieve the spatial direction of the shots. All this information, combined with the range values, allows one to obtain range vectors from the aircraft to the ground points. When these vectors are combined with the aircraft locations they yield accurate coordinates of points on the surface of the terrain (Axelsson, 1998).

Only one GPS ground station within approximately 25 km is required for accurate differential GPS processing. A typical ALS acquisition produces millions of measured points of the ground that allow the generation of high-quality products such as Digital Surface Model (DSM), Digital Terrain Model (DTM), contour plots, etc. The accuracy is of the order of 15 cm in the vertical direction and 50 - 100 cm in the horizontal direction. In addition to elevation information, laser reflectance may be used to generate intensity images to highlight terrain features.

The system records the first and the last laser reflection that, together with INS data, allows the computation of the absolute coordinates of the two points; this feature allows, to some extent, the ALS to acquire data even through a canopy in vegetated areas and provides topographic measurements of the surface underneath (Kraus and Pfeifer, 1998). The ALS resolution and accuracy depends on many factors related to specific construction solutions and technical choices as well as physical and GPS-related limits. Here we briefly analyse the most important physical limits and sources of error.

3. Limits and potentials

The laser beam, though focalised, maintains a physical spread as it propagates. Divergence is a physical property of the laser source fixed by appropriate optical elements in the transmitter. The system ALTM Optech 3033 has a divergence of 0.20 mrad (or 1.0 mrad in divergence beam configuration) therefore the sensor will illuminate a footprint on the ground of ~20 cm from an altitude of 1000 m and ~40 cm from 2000 m (2 m in wide beam mode), the relationship between beam footprint and distance can be described with good approximation as a linear function as reported in Fig. 1. The footprint size is an important feature when considering accuracy and precision. The amplitude of the return signal from a target surface is a function of the integrated energy distribution across the footprint, weighted by the reflectivity profile of the terrain within the footprint. Roughness and slope variations across the footprint complicate this situation, compared to a flat target. In general, non-uniform targets with differences in reflectivity and significant slope across the footprint introduce uncertainty in the actual positioning (both horizontal and vertical) of the target. This situation can be minimized by using systems with the smallest possible divergence, resulting in the smallest footprint on the ground.

Use of the GPS is a key point of ALS mapping. Airborne GPS systems are used in LiDAR to compute the trajectory (state vectors) of the sensor. When performing ALS mapping, it is important to keep in consideration at least the most common GPS related errors that are spread into two main categories.

The first category is carrier phase GPS positioning errors. Differential carrier phase positioning gives centimetre-level accuracy whereas differential code (C/A) positioning gives meter-level accuracy (Baltsavias, 1999). Differential carrier errors strongly affect the final accuracy of ALS products; sources of error include satellite constellation (geometry), satellites availability, orbital errors, multipath, antenna phase centre modelling, and atmospheric errors. Atmospheric errors consist of both tropospheric and ionospheric errors (noise) that can be partly minimized by reducing the distance between master and airborne GPS.

The second category of errors in GPS positioning is related to the geodetic accuracy of the ground control points. The most significant geodetic GPS-related errors are the accuracy of the

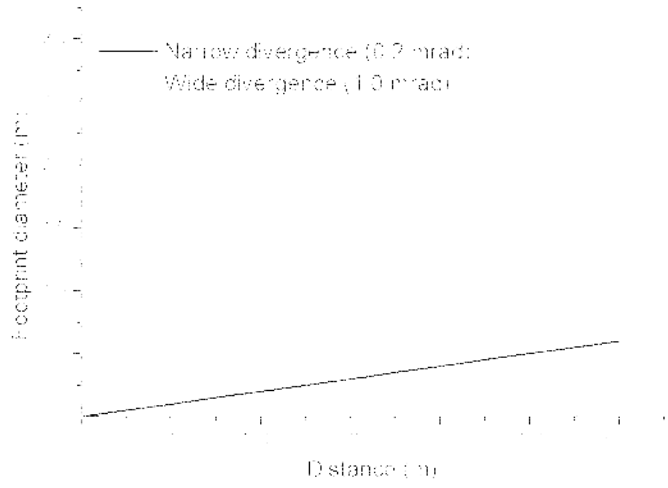

Fig. 1 - Relationship between the footprint diameter and aircraft altitude. In this diagram the target is considered as flat.

model describing the separation between geoid and ellipsoid models. GPS heights are computed onto a specific ellipsoid, whereas practically all engineering and mapping projects are referenced to an orthometric height surface. The accuracy of the geoid models varies from country to country depending on their local geodetic survey offices; for instance, in Italy the Italian vertical datum ITALGEO99 presents an overall consistency at the mean level of ±15 cm (Barzaghi *et al.*, 2002). Vertical GPS error, such as geoid height modelling, will directly influence the accuracy of any ALS product. The computation of the correct orientation of the sensor in space is a necessary condition for calculating an accurate transformation from the local sensor reference frame to the Earth-centred reference frame (WGS84).

Other sources of errors are mainly related to the inertial measurement unit (IMU) system: the orientation of the platform is measured by an on-board IMU that is hard mounted to the LIDAR sensor; the IMU is practically constituted by three laser ring gyroscopes; the specification of the LN200A type we used should guarantee an accuracy of 0.005º pitch/roll, 0.008º heading (POS/AV™ 510 from Applanix – postprocessed solution). This implies that with 0.005º angular error the corresponding positioning error on the ground is 0.17 m at 2000 m. However, there are additional contributions to the angular pointing error that can be only partly minimized by accurate calibration procedures (Optech Inc., undated; Federal Emergency Management Agency, 2000). For instance, there are contributions from the scanning subsystem, due to its own accuracy in measuring the scanner mirror angle and non-linear dynamics in the scanner mirror motion, especially for single-axis. However, it is important to point out that angular errors are actually the sum of many components. On the other hand, all the systematic errors can be minimised by an accurate calibration. The limits of the system in terms of vertical component accuracy can be easily described by analysing the data acquired onto a reference surface and a road which has

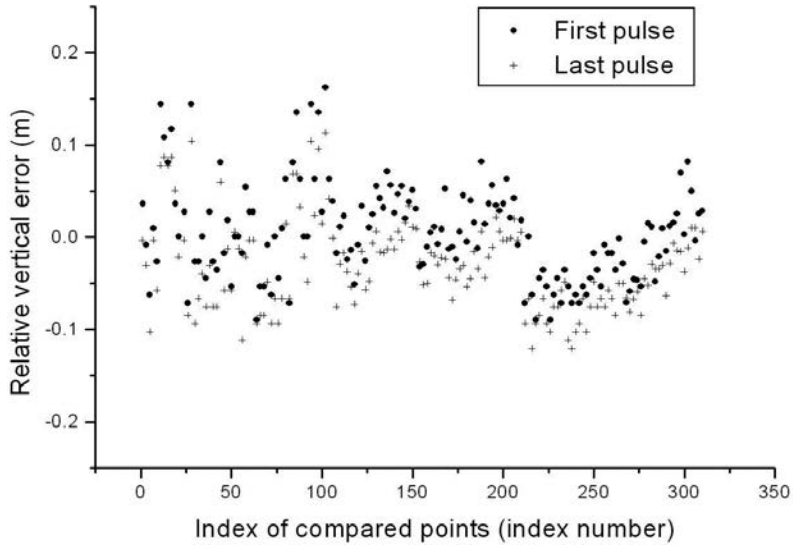

Fig. 2 - Results of the comparison between ALS and surveyed points along the road target. The graph represents the vertical component difference between the surveyed points of the road and the correspondent (within a range of 0.5 m) ALS points.

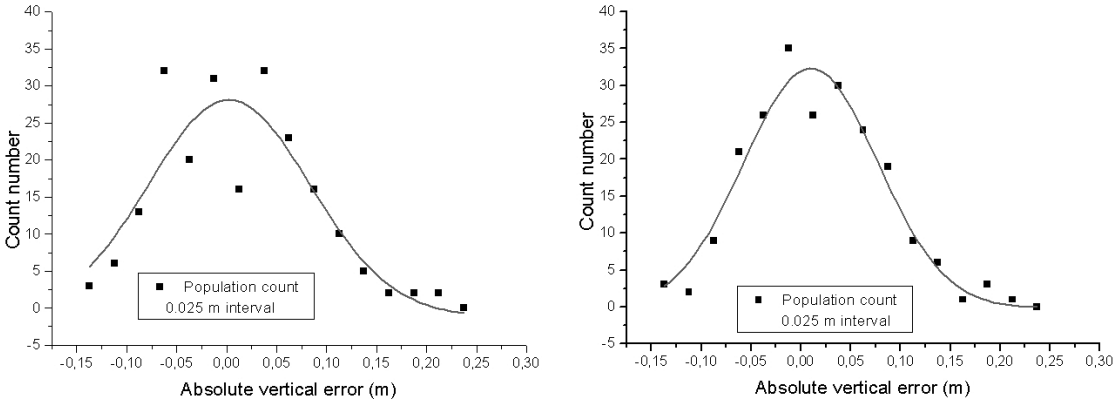

Fig. 3 - Relative error distribution related to the last pulse (left) and first pulse (right). The two figures outline the Gaussian distribution of the error that mathematically justify calibration procedures aimed at keeping the Gaussian bell centred on the origin of error axis.

been measured using differential GPS reference points from which a levelling net was spread; a total of 311 points were measured on the road surface with nominal x,y accuracy of 0.05 m and 0.02 m in z. We acquired ALS data from 1000 m AGL (above ground level) along the road by using 5° of half scan angle and 33 kHz of laser pulse frequency. Data were processed and calibrated according to the constructor standards; the overall GPS RMS error of the state vector solution of the aircraft position was always maintained below 0.037 m. The ALS data volume was drastically reduced after selection of only significant points located within 0.5 m away from the surveyed ones; this population consists in a total of 254 points. The two datasets were then compared and the results are reported in Table 1. The relative errors are shown in Fig. 2, where the data spreading can be outlined; the error distribution referred to the last and first pulse is reported in Fig. 3.

Table 1 - Statistical analysis of the error distribution.

	Mean (m)	Stand. Deviation (m)	Err. Stand. Dev (m)
First pulse	0,01345	+0,06553	+0,00447
Last pulse	0,00633	0,07308	0,00498

4. The application

The main application for laser data is the generation of DSMs, DTMs or other products derived by data classification (Axelsson, 1999). The classification is a semi-automatic process, assigning to every single point a specific class; the classes are generally related to the physical attribute of the targets; typical classes are ground, vegetation, building, (Maas and Vosselman, 1999).

5. The interferometric approach

Satellite radar interferometry involves phase comparison of synthetic aperture radar (SAR) images, gathered at different times with slightly different looking angles. This technique has the potential to detect millimetric target displacements along the Line-Of-Sight (LOS) direction (Massonnet *et al.*, 1993; Massonnet and Feigl, 1998). In fact, a SAR image is a matrix of complex numbers. Amplitude values are related to local reflectivity (the amount of back-scattered energy) while phase values are the sum of two contributions: local reflectivity and a quantity proportional to the sensor-target distance. The aim of the interferometric techniques is to highlight possible range variations of the target, by means of a simple phase difference between two images gathered at different times. In fact, if the local reflectivity remains unchanged in time, its phase contribution disappears in the differentiation, and possible range variations can then be detected. Since the wavelength of the illuminating radiation is usually only a few centimetres (satellite SAR operate in the microwave domain), even a millimetric range variation translates in a phase change of several degrees (Gens and van Genderen, 1996), that can be measured (1 mm corresponds to 13° for ESA-ERS sensors).

Apart from cycle ambiguity problems, limitations are due to temporal and geometrical decorrelation (i.e. the SNR), and to atmospheric artifacts. Temporal decorrelation makes interferometric measurements unfeasible where the electromagnetic profiles and/or the positions of the scatterers change with time within the resolution cell, so that the reflectivity phase contribution cannot be supposed constant with time. The use of short revisiting times proved to be an unsuitable solution, since very slow terrain motion (e.g. seismic fault creeping) cannot be detected. Reflectivity variations as a function of the incidence angle (i.e. geometrical decorrelation) further limit the number of image pairs suitable for interferometric applications, unless the change is reduced due to a point-wise character of the target (e.g. a corner reflector). In areas affected by either kind of decorrelation, generating the interferogram no longer compensates the reflectivity phase contribution, and possible phase variations due to target motion cannot be highlighted. Finally, atmospheric heterogeneity creates an atmospheric phase screen superimposed on each SAR image that can seriously compromise accurate deformation monitoring. Indeed, even considering areas slightly affected by decorrelation, it may turn out to be extremely difficult to discriminate the signal of interest and the atmospheric signature, at least using individual interferograms.

The PSs approach is based on a few observations. Atmospheric artefacts show a strong spatial correlation within every single SAR acquisition, but they are uncorrelated in time. Conversely, target motion is usually strongly correlated in time and can exhibit different degrees of spatial correlation depending on the phenomenon at hand (e.g. subsidence due to water pumping, fault displacements, localized sliding areas, collapsing buildings, etc.). Atmospheric effects can then be estimated and removed by combining data from long time series of SAR images, such as those available in the ESA-ERS archive, gathering data since late 1991. In order to exploit all the available images, and then improve the accuracy of the estimation, only scatterers slightly affected by both temporal and geometrical decorrelation are selected. Possible stable and point-targets, so-called PSs, are then detected on the basis of the stability of their amplitude returns. This allows pixel-by-pixel selection with no spatial averaging. Due to high spatial correlation of the atmospheric contribution, even a sparse grid of measurements may allow proper sampling of

the atmospheric components, provided that the PS density is larger than 3-4 PS/km^2. Of course, a sufficient number of images should be available (usually more than 30), in order to identify PSs and separate the different phase contributions (Ferretti *et al.*, 2000, 2001).

Even though precise state vectors are available for ERS satellites, the orbit indeterminations and their impact on the interferograms cannot be neglected. Estimated APS is actually the sum of two contributions: atmospheric effects and orbital fringes due to baseline errors. However, the latter correspond to low-order phase polynomials and do not change the low-wavenumber character of the signal to be estimated on the sparse PS grid. At the PSs, sub-meter elevation accuracy (due to the wide dispersion of the incidence angles available, usually ± 70 millidegrees with respect to the reference orbit) and millimetric terrain motion detection (due to the high-phase coherence of these scatterers) can be achieved, once atmospheric contributions are estimated and removed. In particular, relative target LOS velocity can be estimated with unprecedented accuracy (sometimes even better than 0.1 mm/yr, due to the long time span). The higher the accuracy of the measurements, the more reliable the differentiations between models of the deformation process under study, a key issue for risk assessment (Colesanti *et al.*, 2003).

The final results of this multi-interferogram approach are the following:

- a map of the PSs identified in the image and their coordinates: latitude, longitude and precise elevation;
- their average LOS velocity;
- the estimated LOS motion component of each PS as a function of time.

Common to all differential interferometry applications, the results are computed with respect to a Ground Control Point (GCP) of known elevation and motion.

6. Limits and potentials

With respect to conventional SAR interferometry, the following advantages should be pointed out.

- Using the PSs technique all the available SAR images recorded by ERS-1 and ERS-2 can be exploited not considering the orbits. On the contrary, only small baselines (i.e. orbits nearby the reference one) should be selected for differential interferometry.
- Single coherent pixel can be identified. This feature is essential in the case of large temporal and geometric baselines, when only point-wise targets provide useful phase information.
- Atmospheric contribution can be estimated and removed, strongly improving measurement accuracy. Target velocity can then be estimated with unprecedented accuracy (up to +/- 0.1 mm/yr) due to exploitation of all the images acquired over the area of interest. Moreover, detection of millimetric motion of the target becomes feasible (at least on a sub-set of PSs exhibiting a very high SNR).
- The high density of measurements, at least in urban areas (>100 PS/km^2) allows a very good spatial sampling that cannot be obtained by means of GPS networks.
- Coarse DEMs can be used in the PSs technique since the accurate elevation of each PS is computed. A better DEM would only reduce the computational time. This is not the case of differential interferometry where the required DEM accuracy is inversely proportional to the normal baseline of the images used for motion detection.

As far as the drawbacks of the technique are concerned, the following limits should be taken into account.

- A large number of images (>25-30) relative to the same track and acquisition mode should be available.
- The processing is computational intensive.
- Even though combining both ascending and descending data a better understanding of the phenomenon under study can be achieved, a full 3D displacement field cannot be recovered (only motion components in the direction of the LOS are measured).
- The density of permanent targets should be high enough (>3 PS/km^2) to carry out the processing.
- Target motion should be slow enough to avoid aliasing due to the sampling period (the repeat cycle of the ERS satellites is 35 days). Usually, if no prior information is available, subsidence rates higher than 7-8 cm/yr cannot be properly estimated.
- Not all the buildings are PSs. If the user is interested in gathering information on a particular site (e.g. a bridge or a dam), it can happen that no PS is present there. In that case, artificial reflectors can be deployed, but the design of a set of ready-to-use solutions to meet user requirements is still in progress.
- Since March 2000, only one satellite, namely ERS-2, can provide the PSs algorithm with useful data. Every fault, damage or breakdown of the on-board systems can compromise the service that should be provided to the users. This is not the case, for example, for GPS data.

7. The application

The analysis of the PSs technique shows that PS data can impact on the following fields:

- detection and monitoring of urban subsidence due to natural or anthropogenic causes;
- volcanic areas and seismic faults monitoring (non heavily vegetated areas);
- landslide monitoring;
- stability check of buildings (whenever at least one PS is available on the target of interest).

The probability of success in performing these different tasks depends on various factors, such as: (1) the number of data available; (2) the location of the area of interest (e.g. rural or urban context); (3) the PS density; (4) the motion of the targets. In any case, the results of the research carried out by the SAR Group of the Politecnico of Milan have shown how PS data can play a major role in urban subsidence monitoring, where PS density and temporal sampling are well suited for the spatial and temporal characteristics of the phenomena. Surely enough, without the deployment of artificial reflectors, PS data will have weaker impact on landslide and slope instability monitoring, due to the low density of measurement points and the highly unpredictable behaviour of terrain motion. As far as volcanoes and seismic fault monitoring is concerned, certainly the results obtained on southern California and the comparison with GPS data have clearly shown how PS data can offer a new tool for seismologists. Indeed the measurement density is an order of magnitude higher than what can be achieved with GPS networks. On the other hand, since the displacement fields that can be estimated are 1D and not 3D, PS data will not substitute GPS measurements, but probably both technologies will be used in the near future to feed more accurate mathematical models of geophysical phenomena. Though the use of PS

data for building stability check could be considered as a real breakthrough toward collapse prevention, it should be pointed out that further studies are still needed to identify the best strategy to "transform every roof into a PS". Of course, needless to say, the potential market would be huge, but several constraints (e.g. environmental impact of the reflectors, maximum density of reflectors to avoid radar saturation, best processing chain to manage and update millions of PSs and to provide a service on national scale) have to be satisfied. Both the technical analysis of the PSs data and the results of the interviews with different user groups and experts in geodetic surveys have highlighted how the PSs technique can be considered at present the most powerful tool available for land subsidence monitoring in urban areas. In fact, the millimetric accuracy together with the high spatial sampling and a historical archive from 1991 allows unprecedented subsidence analyses. Due to the importance of this topic, the following section will be entirely devoted to an overview of subsidence and a brief outline of the potential market related to these phenomena. Surely enough, the PSs technique will play a major role there.

8. The digital image

The photographic data set was acquired with a 4x4k pixel digital camera mounted onboard the helicopter where the ALS system is located. The radiometric dynamic of the camera is 16 bit for every single RGB channel, the optic is a 50 mm that gives an aperture of 40° which completely overlaps the laser swath. The orthorectification process is performed using the state vector of the airborne platform computed in the focal position and the attitude valued derived by the inertial system (King, 1995). The camera calibration parameters are derived by estimation of common points in overlapping images. The reference digital surface model adopted for the orthorectification is the model key point of the ground data. The final product is a geocoded image formed by mosaicking of approximately 16 images; the ground resolution is 7 cm.

9. The case history of Palmanova

The town of Palmanova (northeastern Italy) was selected as test-site; in this area we acquired a full laser scan, photographic and ERS1 and ERS2 synthetic aperture radar data sets; the three data sets were then fused together following the scheme reported in Fig. 4.

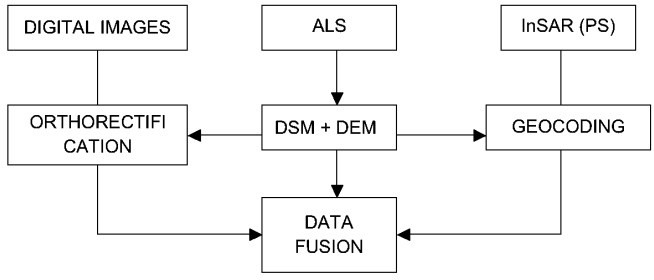

Fig. 4 - Bloch diagram describing the processing chain adopted for the data fusion of the three data set: laser scan, photographic and PSs.

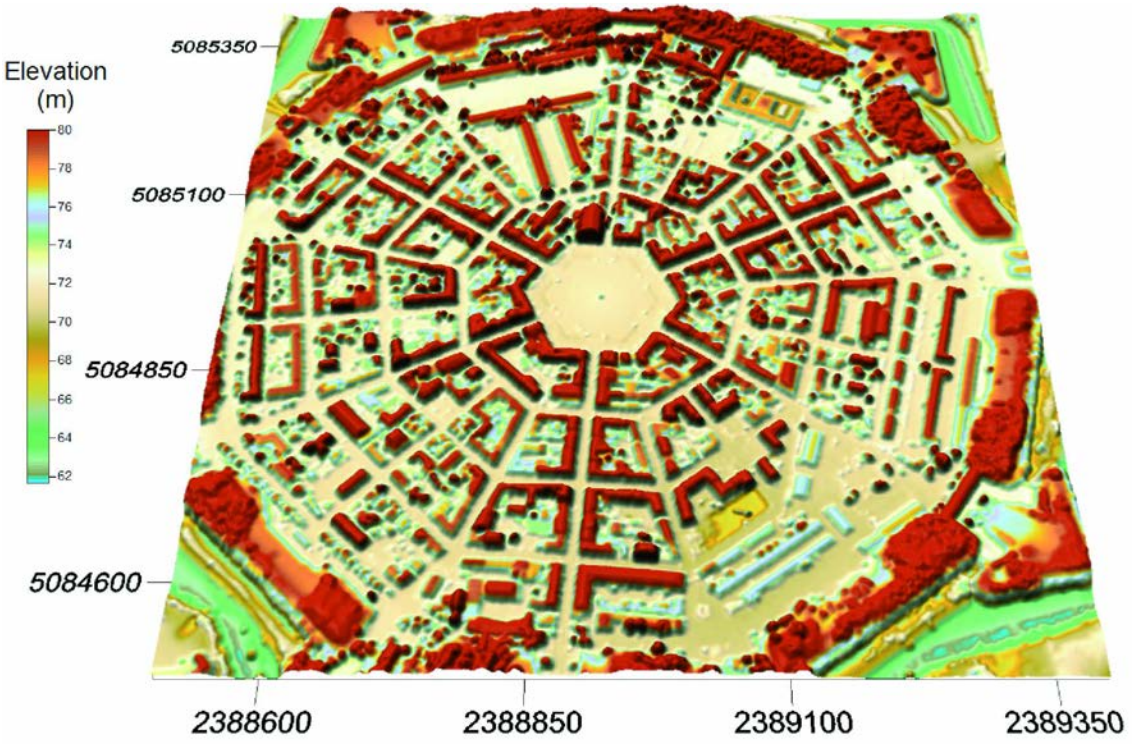

Fig. 5 - Laser scan digital surface model.

The entire area of Palmanova has been covered by a laser scan acquisition and a contemporary aerophotographic acquisition. The laser scan acquisition was performed from an altitude of 1000 meters above ground level with a nominal density of 1 point/m^2 ; the data were then gridded on a regular matrix with 1m x 1m square cell using triangulation with linear interpolation algorithms. The final result is the image represented in Fig. 5.

A series of digital images were acquired on the same area and orthorectified onto the ground model derived by classification of the laser data. The orthorectification was conducted using the positioning and attitude information derived by the navigation system mounted onboard the helicopter and used for the laser scan. The result is shown in Fig. 6 where the orthoimages have been mosaicked together and draped onto the digital surface model derived by laser scan data.

The interferometric processing has been conducted thanks to the ERS-SAR data set (track 351, frame 2673, descending acquisition mode) available in the ESA archive. In Table 2, a summary description of the data set is given: for each image the platform number (ERS-1, ERS-2), the normal and temporal baselines with respect to the master acquisition, are given; in this table, the master image is highlighted in bold font. After the choice of the master acquisition, based on the dispersion of the normal and temporal baselines of the other images (slaves) and after the focusing process, the PSs technique proceeds with the computation of the interferometric phases. Such values describe the point behaviour, in terms of topography, deformation rate plus all the noise contributions. In order to isolate the topography and

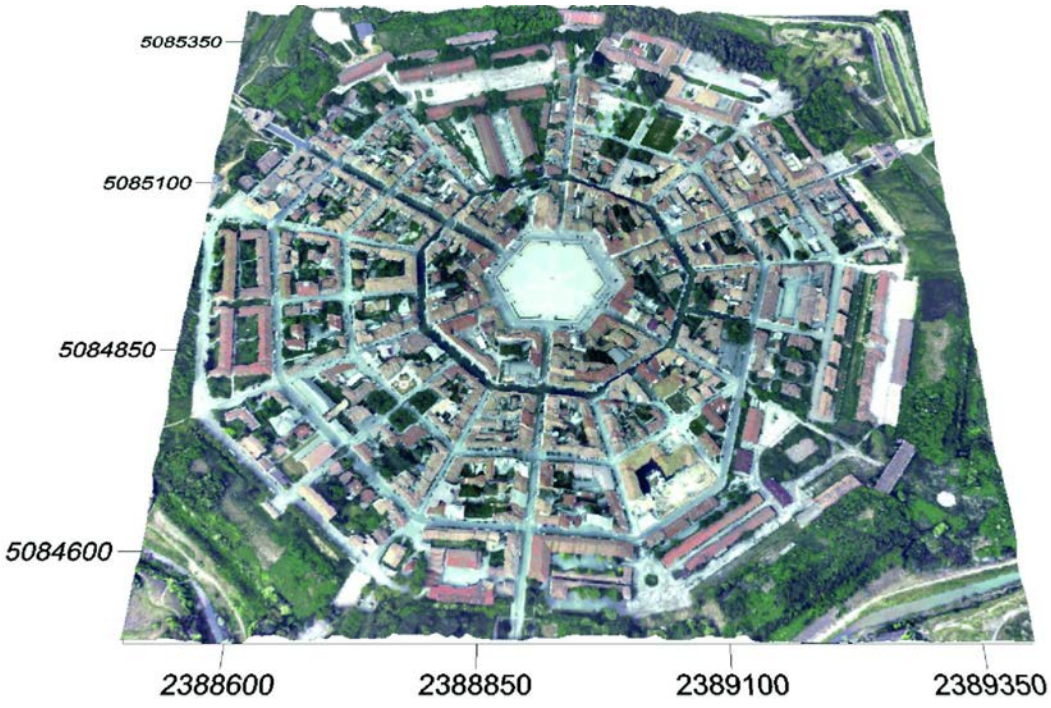

Fig. 6 - Orhtoimages mosaicked and draped onto the laser scan DEM.

Fig. 7 - PSs, orthoimages and laser scan fused together. LIDAR DEM and PS integration. Full integration among laser scan digital elevation model, orthoimages and terrain (buildings) deformation (expressed in mm/year) derived by application of PSs technique.

deformation contributions from the atmosphere phase screen (APS), we first selected those points whose behaviour is not very sensitive to the particular acquisition time and baseline: the PSs. The atmospheric residue is then estimated over these points and then removed from the data.

About 1,000 PSs have been detected in the Palmanova area. For each PS it is possible to estimate its elevation with a nominal precision of about 1 m. The LIDAR DEM has then be used to integrate the result. PS-SAR data show an overall agreement with LIDAR samples; the overall image of this fusion process is shown in Fig. 7. The integration of LIDAR and PS-SAR results suggests a relation between the volumetry of the scattering centre and its velocity.

Table 2 - Track 351, Frame 2673 dataset.

Date	Platform	Bn (m)	Bt (days)	Date	Platform	Bn (m)	Bt (days)
19920421	1	208.47	-2404.0	19970926	2	-284.05	-420.0
19920526	1	-856.35	-2369.0	19971031	2	-966.26	-385.0
19920804	1	-201.83	-2299.0	19971205	2	50.84	-350.0
19920908	1	209.78	-2264.0	19980109	2	-381.32	-315.0
19921013	1	183.07	-2229.0	19980320	2	-155.73	-245.0
19921117	1	-437.60	-2194.0	19980424	2	13.65	-210.0
19930126	1	-437.29	-2124.0	19980529	2	-143.37	-175.0
19930406	1	454.95	-2054.0	19980703	2	-827.36	-140.0
19930615	1	-592.78	-1984.0	19980806	1	207.62	-106.0
19931102	1	355.84	-1844.0	19980807	2	-228.13	-105.0
19931207	1	555.97	-1809.0	19980911	2	-293.43	-70.0
19950330	1	-1041.16	-1331.0	19981016	2	-401.87	-35.0
19950504	1	-862.44	-1296.0	**19981120**	**2**	**0.00**	**0.0**
19950608	1	-309.11	-1261.0	19981225	2	-460.81	35.0
19950609	2	-447.89	-1260.0	19990304	1	-1054.03	104.0
19950713	1	-517.82	-1226.0	19990305	2	-1220.69	105.0
19950818	2	-117.28	-1190.0	19990409	2	246.27	140.0
19950921	1	-481.15	-1156.0	19990514	2	148.38	175.0
19951026	1	531.71	-1121.0	19990618	2	-421.54	210.0
19951027	2	602.11	-1120.0	19990723	2	369.40	245.0
19960104	1	3.67	-1051.0	19990827	2	-1262.66	280.0
19960314	1	151.50	-981.0	19991001	2	98.05	315.0
19960315	2	117.65	-980.0	19991105	2	-448.32	350.0
19960418	1	246.56	-946.0	20000113	1	-1117.19	419.0
19960419	2	165.62	-945.0	20000114	2	-960.36	420.0
19960524	2	-302.40	-910.0	20000217	1	-695.26	454.0
19960627	1	-51.00	-876.0	20000218	2	-656.18	455.0
19960628	2	-162.14	-875.0	20000428	2	305.10	525.0
19960802	2	-58.20	-840.0	20000602	2	-393.29	560.0
19960906	2	-549.36	-805.0	20000707	2	-545.28	595.0
19961011	2	-496.87	-770.0	20000811	2	136.54	630.0
19961115	2	973.44	-735.0	20000915	2	-273.33	665.0
19961220	2	-606.97	-700.0	20001020	2	-112.58	700.0
19970228	2	-237.79	-630.0	20001124	2	588.02	735.0
19970509	2	-369.29	-560.0	20001229	2	-614.91	770.0
19970718	2	-313.68	-490.0	20020222	2	255.40	1190.0
19970822	2	113.20	-455.0	20020712	2	-730.81	1330.0

10. Conclusions

This case history demonstrates how to generate large remote sensed data sets of the territory, taking into account its geometric, radiometric and dynamic aspects. The overall impact of the integration of all these data in a GIS is relevant to many different fields of application such as: landslide monitoring, infrastructure analysis, single-building stability check. In the future, the availability and the lower cost of both LIDAR and PS data will allow a large-scale application of these technologies that will probably change the scenario of land management completely. Powerful Decision Support Systems capable of providing effective and reliable information for Civil Protection applications will become a standard system, while historical data sets will provide a brand new set of data for tectonics and geodynamics. Finally, final users will have real benefits from a new set of remote sensing technologies.

REFERENCES

Ackermann F.. 1999: *Airborne laser scanning present status and future expectations*. ISPRS J. of Photogrammetry and Remote Sensing, **54**, 64-67.

Axelsson P.; 1998: *Integrated sensors for platform orientation and topographic data acquisition*. In: Proceedings of the Symposium on Digital Photogrammetry, Istanbul, Turkey, pp. 1-11.

Axelsson, P.; 1999: *Processing of laser scanner data - algorithms and applications.* ISPRS J. of Photogrammetry and Remote Sensing, **54**, 138-147.

Baltsavias E.P.; 1999: *Airborne laser scanning: basic relations and formulas.* ISPRS J. of Photogrammetry and Remote Sensing, **54**, 199-214.

Barzaghi R., Betti B., Borghi A., Sona G. and Tornatore V; 2002: *The Italian quasi-geoid ITALGEO99*. Bollettino di Geodesia e Scienze Affini, **61**, 35-51.

Colesanti C., Ferretti A., Novali F., Prati C. and Rocca F.; 2003: *SAR monitoring of progressive and seasonal ground deformation using the permanent scatterers technique*. IEEE Trans. on Geoscience and Remote Sensing, **41**, 1685-1701.

Federal Emergency Management Agency; 2000: *Appendix 4B. Airborne Light Detection and Ranging Systems.* Flood Insurance Study Guidelines and Specifications for Study Contractors. http://www.fema.gov/fhm/gs_main.shtm, updated 12/5/2005.

Ferretti A., Colesanti C., Prati C. and Rocca F.; 2001: *Non-linear subsidence rate estimation using permanent scatterers in differential SAR interferometry*. In: Proceedings of the Joint IEEE/ISPRS Workshop on remote sensing and data fusion over urban areas, Roma, 8-9 November 2001, pp. 52.

Ferretti A., Prati C. and Rocca F.; 2000: *Measuring subsidence with SAR Interferometry: applications of the permanent scatterers technique*. In: Proceedings of the 6th International Symposium on Land Subsidence, Vol. II, SISOLS2000, 24-29 September 2000, Ravenna, pp. 67-79.

Gens R. and van Genderen J.L; 1996: *SAR interferometry - issues, techniques, applications*. International J. for Remote Sensing, **17**, 1803-1835.

Hill J.M., Graham L.A. and Henry R.J.; 2000: *Wide-area topographic mapping and applications using airborne light detection and ranging (LIDAR) Technology.* Photogrammetric Engineering and Remote Sensing, **66**, 908-914.

King D.J.; 1995: *Airborne multispectral digital camera and video sensors: a critical review of system designs and applications*. Canadian J. of Remote Sensing, **21**, 245-273.

Kraus K. and Pfeifer N.; 1998: *Determination of terrain models in wooded areas with airborne laser scanner data*. ISPRS J. of Photogrammetry and Remote Sensing, **53**, 193-203.

Maas H.-G. and Vosselman G.; 1999: *Two algorithms for extracting models from raw laser altimetry data*. ISPRS J. of Photogrammetry and Remote Sensing, **54**, 153-163.

Massonnet D. and Feigl K.L.; 1998: *Radar interferometry and its application to changes in the earth's surface*. Reviews of Geophysics, **36**, 441-500.

Massonnet D., Rossi M., Carmona C., Adragna F., Peltzer G., Feigl K. and Rabaute T.; 1993: *The displacement field of the Landers earthquake mapped by radar interferometry.* Nature, **364**, 138-142.

Optech Inc.; undated: ALTM 3033 User Manual, pp. 121-126.

Corresponding author: Franco Coren
Istituto Nazionale di Oceanografia e di Geofisica Sperimentale - OGS,
Dipartimento di Geofisica della Litosfera;
Borgo Grotta Gigante 42/c, Sgonico (Trieste), Italy
phone: +39 0402140255; fax: +39 040327307; e-mail: fcoren@ogs.trieste.it